A Cost-Effective Method to Prepare Gold Nanoparticles from Pomegranate Fruit Peel; Assessing their *in vitro* Pharmacological Activity

Türkan Mutlu Yar [a], Ayşe Baran,[b] Mahmut Yıldıztekin [c,*] Ülkü Karaman [a], and Sevgi İrtegün Kandemir [d]

* *Corresponding author: mahmutyildiztekin@mu.edu.tr*

DOI: 10.15376/biores.21.4.9947-9961

GRAPHICAL ABSTRACT

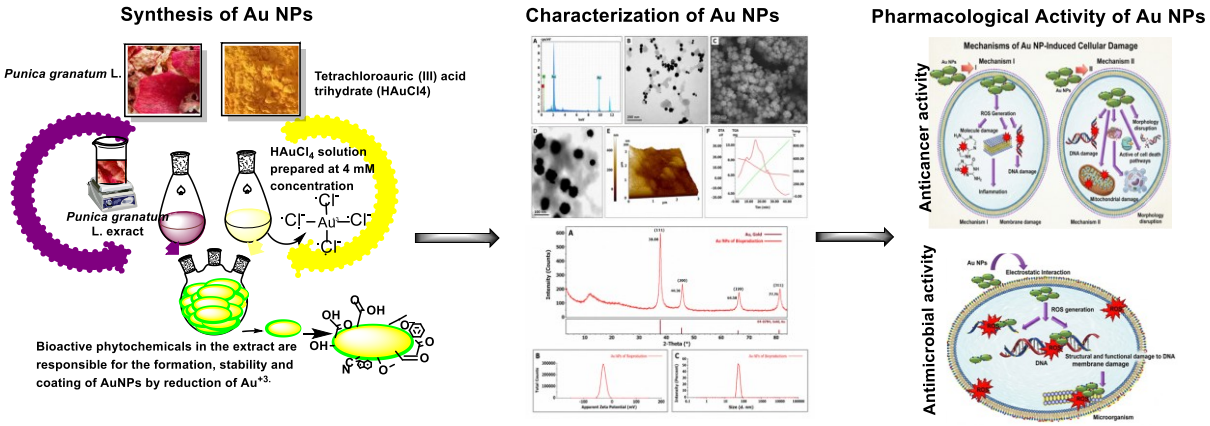

A Cost-Effective Method to Prepare Gold Nanoparticles from Pomegranate Fruit Peel; Assessing their *in vitro* Pharmacological Activity

Türkan Mutlu Yar [a], Ayşe Baran,[b] Mahmut Yıldıztekin [c,*] Ülkü Karaman [a], and Sevgi İrtegün Kandemir [d]

A rapid, eco-friendly, and cost-effective green synthesis route was established for the fabrication of gold nanoparticles (Au NPs) utilizing aqueous extracts derived from *Punica granatum* L. (pomegranate) agricultural peel waste, thereby valorizing agro-industrial by-products. The proposed method eliminates the need for hazardous reducing agents and external stabilizers, offering a fully biogenic and waste-to-value nanomanufacturing approach. The synthesized AuNPs were extensively characterized using UV–Vis spectroscopy, FTIR, XRD, TEM, STEM, DLS, zeta potential analysis, and EDX, confirming the formation of crystalline, spherical, and highly stable nanoparticles with a surface plasmon resonance peak at 532.3 nm, an average hydrodynamic diameter of 47.1 nm, and a zeta potential of −16.2 mV. The integration of multiple complementary analytical techniques further validated the structural and colloidal stability of the nanostructures. The AuNPs exhibited strong, dose-dependent antimicrobial activity against pathogenic microorganisms and significant cytotoxic effects against human cancer cell lines *in vitro*. The novelty of this work lies in the dual contribution of (i) transforming agricultural waste into a functional nanomaterial platform and (ii) producing biologically active AuNPs *via* a single-step, green, and scalable synthesis route without chemical additives.

DOI: 10.15376/biores.21.4.9947-9961

Keywords: Au NPs; Green synthesis; Nanoparticles; Pharmacological agents; Pomegranate

Contact information: a: Faculty of Medicine, Department of Parasitology, Ordu University, Ordu, Türkiye; b: Field Crops Department, Kiziltepe Faculty of Agricultural Sciences and Technologies, Mardin Artuklu Universıty, Mardin 47200, Türkiye; c: Department of Herbal and Animal Production, Koycegiz Vocational School, Mugla Sıtkı Kocman University, Mugla 48000, Türkiye; d: Department of Medical Biology, Dicle University Central Research Laboratory, Faculty of Medicine, Dicle University, Diyarbakir, Türkiye;
** Corresponding author: mahmutyildiztekin@mu.edu.tr*

INTRODUCTION

Nanoparticles, which are typically defined by dimensions ranging from 1 to 100 nm, have become a cornerstone of contemporary materials research due to their unique properties, including high surface-area-to-volume ratios, superior conductivity, and tunable energy bands. These characteristics facilitate their application across various sectors, such as electronics, optics, sensors, and the food industry. In biomedical research, gold nanoparticles are particularly valued for their efficacy in drug delivery, as well as antibacterial and anticancer applications. These clinical advantages are primarily attributed to their exceptional optical properties, biological compatibility, and ease of

surface modification (Al-Radadi 2023; Ullah *et al.* 2024; Baran 2025). While multiple methods exist for Au NP synthesis, green synthesis presents a superior, eco-friendly alternative to traditional physicochemical strategies. This biogenic approach reduces the dependence on hazardous chemicals, thereby minimizing environmental impact while enhancing cost-effectiveness and energy efficiency. Additionally, green-synthesized Au NPs demonstrate high biocompatibility, excellent yield, and sustainable sourcing (Baran 2023; Döll *et al.* 2023; Niżnik *et al.* 2024). This methodology utilizes various plant materials—such as leaves, flowers, fruits, or roots—as precursors. Phytochemicals present in these extracts, particularly phenolic acids and flavonoids, act as active reducing agents to convert trivalent gold ions (Au^{3+}) into metallic nanoparticles, while concurrently stabilizing the synthesized Au NPs (Ullah *et al.* 2024; Baran 2025).

Punica granatum L. (pomegranate), belonging to the Lythraceae family, is an ancient fruit tree that thrives in tropical and subtropical regions. Historically derived from the Latin *Malum granatum* ('seeded apple'), the tree is characterized by a contorted stem, elongated leaves, and vibrant orange or crimson flowers. Exhibiting remarkable climatic adaptability, the tree produces spherical fruits (6 to 12 cm in diameter) with peels ranging in color from yellow and green to pink (Al-Zoreky 2009; Valero-Mendoza *et al.* 2023). Pomegranate peel possesses a complex biochemical profile, including proteins, polysaccharides, and essential minerals, alongside high concentrations of phenolic compounds such as flavonoids, hydrolyzable tannins, and phenolic acids. Scientific literature has consistently demonstrated the broad-spectrum bioactivity of pomegranate peel extract, including its antioxidant, anticancer, anti-inflammatory, neuroprotective, antiviral, and antibacterial properties (Negi and Jayaprakasha 2003; Zahin *et al.* 2010; De Trovão *et al.* 2023; Scaglione *et al.* 2024).

Numerous studies have reported the green synthesis of Au NPs using extracts obtained from different parts of *Punica granatum* L., including leaves, fruits, and peels collected from various geographical regions. These studies have demonstrated that the phytochemical composition of the plant material plays a crucial role in determining the physicochemical characteristics of the synthesized nanoparticles, leading to significant variations in particle size, morphology, crystal structure, colloidal stability, and biological activity. In particular, AuNPs synthesized using pomegranate peel extracts have attracted considerable attention because of their remarkable antioxidant, drug delivery, and photocatalytic properties (Franzolin *et al.* 2022; Kharey *et al.* 2023; Serdar 2024; Niaz *et al.* 2026). Nevertheless, most of these studies have primarily focused on nanoparticle synthesis and physicochemical characterization, while comprehensive investigations of their biological activities remain limited. Moreover, only a few studies have evaluated multiple biological functions within a single experimental framework.

The present study differs from previous reports in several important aspects. First, the *Punica granatum* L. plant material was collected from a different geographical region, which may influence its phytochemical profile and, consequently, the characteristics of the synthesized nanoparticles. Second, a distinct green synthesis strategy was employed, resulting in AuNPs with unique physicochemical properties, including differences in particle size, morphology, and surface chemistry. These characteristics were systematically correlated with their biological performance. Furthermore, beyond detailed physicochemical characterization, the synthesized AuNPs were comprehensively evaluated for their cytotoxic effects against different cancer cell lines and their antimicrobial activities against pathogenic bacterial and yeast strains. By integrating extensive physicochemical characterization with broad biological evaluation,

this study provides new insights into the structure–activity relationships of *Punica granatum*-derived AuNPs and is expected to make a meaningful contribution to the development of plant-mediated gold nanoparticles for biomedical applications.

The objective of this study was to develop a novel, eco-friendly approach for synthesizing gold nanoparticles using agricultural waste extracts of pomegranate sourced from the Bismil region of Diyarbakır. Furthermore, this work characterizes the physicochemical properties of the synthesized Au NPs and evaluates their therapeutic potential as biomedical agents.

EXPERIMENTAL

Materials and Methods

Preparation of extract and tetrachloroauric acid trihydrate solution for synthesis medium

Waste pomegranate peels obtained from a local market in Batman were cleaned with tap and distilled water to remove impurities. A 100 g sample of the purified waste was extracted in 500 mL of distilled water at 45 °C for 30 min without prior drying. The resulting extract was cooled to ambient temperature and filtered for Au NP synthesis. A solid compound of tetrachloroauric acid trihydrate ($HAuCl_4 \cdot 3H_2O$) from Kandel, Germany, branded as Alfa Aesar, was used as the metal source for producing Au NPs. A metal solution with a concentration of 4 mM has been created using this chemical for the creation of Au NPs.

Fresh waste pomegranate peels (100 g, Batman, Turkey) were washed, extracted in 500 mL of distilled water at 45 °C for 30 min without drying, cooled, and filtered. The resulting extract was then mixed with a 4 mM aqueous solution of tetrachloroauric (III) acid trihydrate ($HAuCl_4.3H_2O$; Alfa Aesar, Germany) for Au NP synthesis.

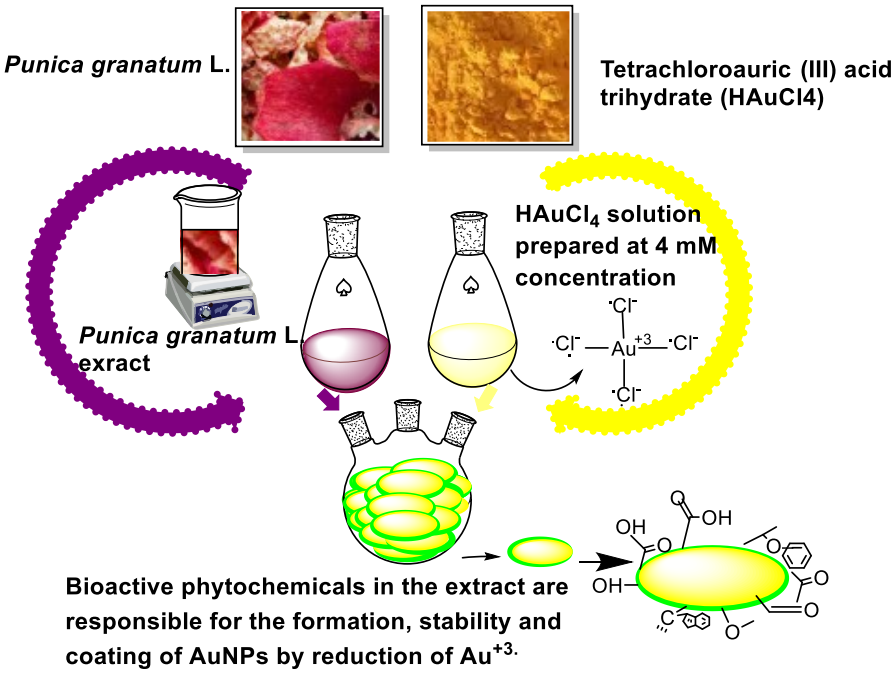

Fig. 1. A representative schematic of the synthesis mechanism of gold nanoparticles using extract obtained from pomegranate peel

Synthesis of Au NPs

For nanoparticle fabrication, equal volumes of the pomegranate extract and 4 mM $HAuCl_4$ were blended under continuous agitation (150 rpm, 50 °C) for an hour. Initial Au NP synthesis was verified by a rapid color transformation within five min and subsequently monitored *via* spectrophotometric tracking. To isolate the stable colloidal nanoparticles for therapeutic evaluation, the mixture underwent centrifugation at 6000 rpm for 20 min, followed by consecutive distilled water washes and final desiccation at 70 °C (Fig. 1).

Characterization of Au NPs

The synthesis and optical traits of the Au NPs were verified *via* ultraviolet-visible (UV-vis) spectrophotometry (Perkin Elmer) across a 300 to 800 nm scanning range to pinpoint the Surface Plasmon Resonance (SPR) maxima. The hydrodynamic dimensions and zeta potential were evaluated using the Zeta Sizer from (Malvern). The thermal behavior was determined by thermogravimetric analysis (TGA) (Shimadzu TGA-50). Chemical interactions and functional groups driving Au^{+3} bioreduction and subsequent nanoparticle capping were resolved through Zeta sizer, ultraviolet-visible spectroscopy (UV–Vis), and Fourier-transform Infrared Spectroscopy (FTIR) (4000 to 500 cm^{-1}). Topography and surface morphologies were comprehensively investigated using Atomic Force Microscopy (AFM). Elemental profiles and crystal phases were established using Energy-Dispersive X-ray Spectroscopy (EDX) and X-ray Diffraction (XRD) (Rigaku Miniflex). These observations were supplemented by transmission electron microscopy (TEM), scanning transmission electron microscopy (STEM), and field emission scanning electron microscopy (FE-SEM) monitoring, where the average crystallite size was determined from the full width at half maximum (FWHM) values *via* the Debye-Scherrer formula (Li *et al.* 2024).

Potential Medical Agent of Au Nanoparticles

Anticancer effects of Au NPs

The cytotoxicity of the biosynthesized Au NPs was evaluated *via* MTT (3-(4,5-dimetiltiyazol-2-il)-2,5-difeniltetrazolyum bromür) colorimetric assay against Caco-2, U118, Skov-3, and healthy cell lines at Dicle University. The cells were maintained under standard incubation parameters (37 °C, 5% CO_2) and transferred to 96-well culture plates upon achieving 80% confluence. After exposing the cells to varying concentrations of Au NPs for a 24 h period, the MTT reagent and Dimethyl sulfoxide (DMSO) were introduced, and spectrophotometric absorbance was quantified at 540 nm. Percent cell viability was computed using the equation (U/C) x 100, where "U" and "C" denote the optical densities of the treated groups and untreated controls, respectively (Irtegun Kandemir and İpek 2018).

Antimicrobial activities

The antimicrobial efficacy of the biosynthesized Au NPs was investigated against *Candida albicans*, *Escherichia coli*, and *Bacillus subtilis via* the broth microdilution method to establish their minimum inhibitory concentrations (MICs). The microbial cultures, sourced from Dicle University, were grown overnight at 37 °C on nutrient agar and Sabouraud dextrose agar slants. Following incubation, the microbial density was standardized to a 0.5 McFarland turbidity threshold as described by İpek *et al.* (2024). Inoculations were performed in sterile 96-well microplates containing Mueller–Hinton

broth for the bacterial strains and RPMI 1640 medium for the fungal strain. The inhibitory potential of the Au NP aqueous suspensions was benchmarked against a 2 mM $HAuCl_4$ solution and reference antimicrobials (Fluconazole, Vancomycin, and Colistin). Following a 24-h incubation period at 37 °C, the MIC endpoints were recorded as the lowest concentrations that induced complete visual suppression of microbial proliferation.

RESULTS AND DISCUSSION

Characterization Data of Au NPs

UV-vis data and FTIR data of Au NPs

The successful reduction of gold ions was initially indicated by a visible color shift from pink to red within 30 min of mixing the pomegranate peel extract with $HAuCl_4$. Subsequent UV–Vis analysis throughout the 60-min reaction period revealed a well-defined surface plasmon resonance peak at 532.3 nm, establishing the formation of stable Au NPs (Fig. 2a) (Pechprakob *et al.* 2023).

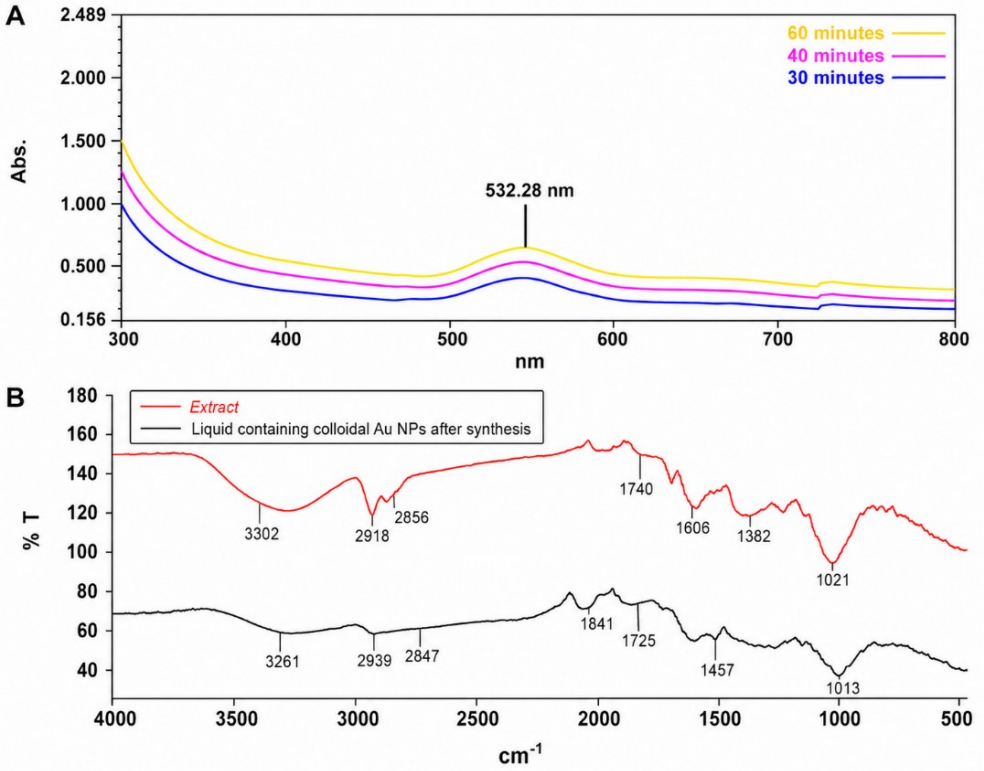

Fig. 2. (a) UV–Vis absorption spectra of biosynthesized Au NPs showing the maximum SPR wavelength; (b) FTIR spectra of the resulting colloidal Au NP suspension

The FTIR spectroscopy was employed to identify the biogenic functional groups within the pomegranate waste extract and elucidate their specific roles in the synthesis, capping, and surface modification of the Au NPs. The distinctive spectral shifts detected at 3302, 2918, and 2855 cm^{-1} confirm that (O–H) and alkene (–C=C–) stretching vibrations are directly involved in the bioreduction of Au^{3+} ions. Furthermore, the prominent shifts observed at 1740, 1606, and 1382 cm^{-1} demonstrate the active

participation of oxygen- and nitrogen-containing functional groups in the capping and subsequent stabilization of the fabricated nanoparticles (Fig. 2b) (Franzolin *et al.* 2022; Niaz *et al.* 2026).

Crystal structures data of Au NPs

The crystal structure, surface charge, and size distribution profiles of the synthesized Au NPs were characterized using XRD and DLS analyses. The XRD patterns, illustrated within the 2θ range of 20 to 80° in Fig. 3a, revealed four distinct Bragg reflections at 38.08°, 44.36°, 64.58°, and 77.76°. These peaks correspond to the (111), (200), (220), and (311) crystallographic planes of the face-centered cubic gold structure, aligning precisely with the JCPDS card no. 04–0784 (Baran 2025). Based on the Full Width at Half Maximum (FWHM) value of the prominent (111) reflection, the average crystallite size was determined as 6.2 nm *via* the Debye-Scherrer equation. This crystalline size is highly consistent with similar green synthesis literature; for instance, Suriyakala *et al.* (2022) estimated a crystallite size of 6.9 nm for Au NPs derived from *Jatropha integerrima* Jacq. extract.

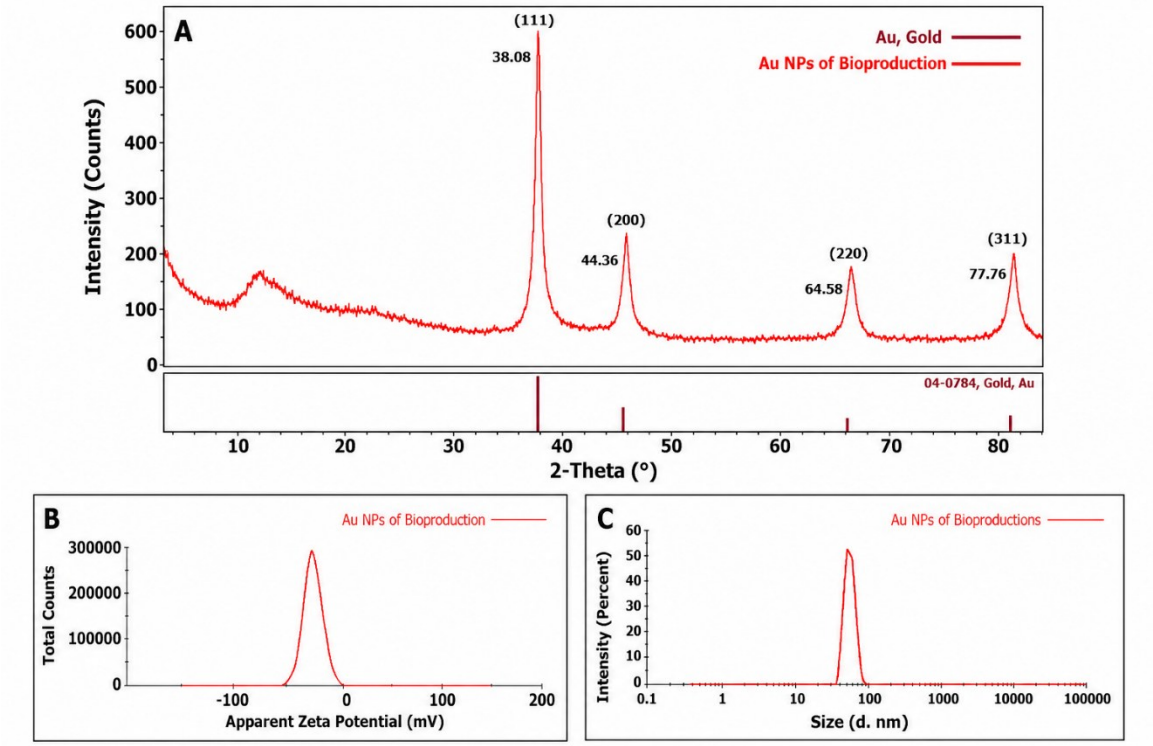

Fig. 3. XRD and DLS data of Au NPs produced from pomegranate from fruit peels extract: **(a)** crystal structures, **(b)** Surface charge, and **(c)** hydrodynamic size distributions

Surface structure and morphology data of Au NPs

The electrostatic stability of the colloidal gold was evaluated through DLS zeta potential measurements (Fig. 3b), which yielded an average surface charge of –16.2 mV. The entirely negative surface charge of the nanoparticles plays a key role in preventing aggregation and fluctuations, thereby ensuring long-term colloidal stability. This negative net charge is primarily attributed to the capping effect of the phytochemicals present in the plant extract. Similar surface charge behaviors have been reported in green synthesis

frameworks, with zeta potentials around –19 mV observed in related literature (Dubey *et al.* 2013; Kumar *et al.* 2018; Baran 2025).

Comprehensive morphological features, thermal behavior, and elemental composition of the Au NPs were further elucidated using TEM, FESEM, AFM, EDX, and TGA-DTG techniques. SEM images showed that the nanoparticles clustered on the surface, forming grape-cluster-like aggregates. This can be explained by Van der Waals attraction forces and the influence of biomolecules, which are commonly observed in green synthesized nanoparticles. Despite the aggregation, it is clearly apparent that the particles were nano-sized. At higher magnification, the majority of the particles appeared to be spherical and have smooth edges. Some particles were observed to be in contact with each other, forming larger structures. The approximate particle size was around 20 to 50 nm. Furthermore, TEM and SEM analyses revealed that the nanoparticles mostly had a spherical morphology and exhibited partial agglomeration. AFM analysis showed that the surface topography was non-homogeneous, but the nanoparticles were effectively distributed on the surface. TGA/DTA results support the presence of organic phytochemicals coating the nanoparticle surface during green synthesis and the good thermal stability of the synthesized Au NPs at high temperatures (Fig. 4a to 4e) (Adem *et al.* 2024; Baran *et al.* 2025; Niaz *et al.* 2026). These morphological attributes strongly mirror previous green synthesis reports; spherical configurations have likewise been documented for Au NPs synthesized using *Nepeta bodeana* extracts (Sharifi-Rad *et al.* 2024) and *Curcuma longa* extracts (Xie *et al.* 2024).

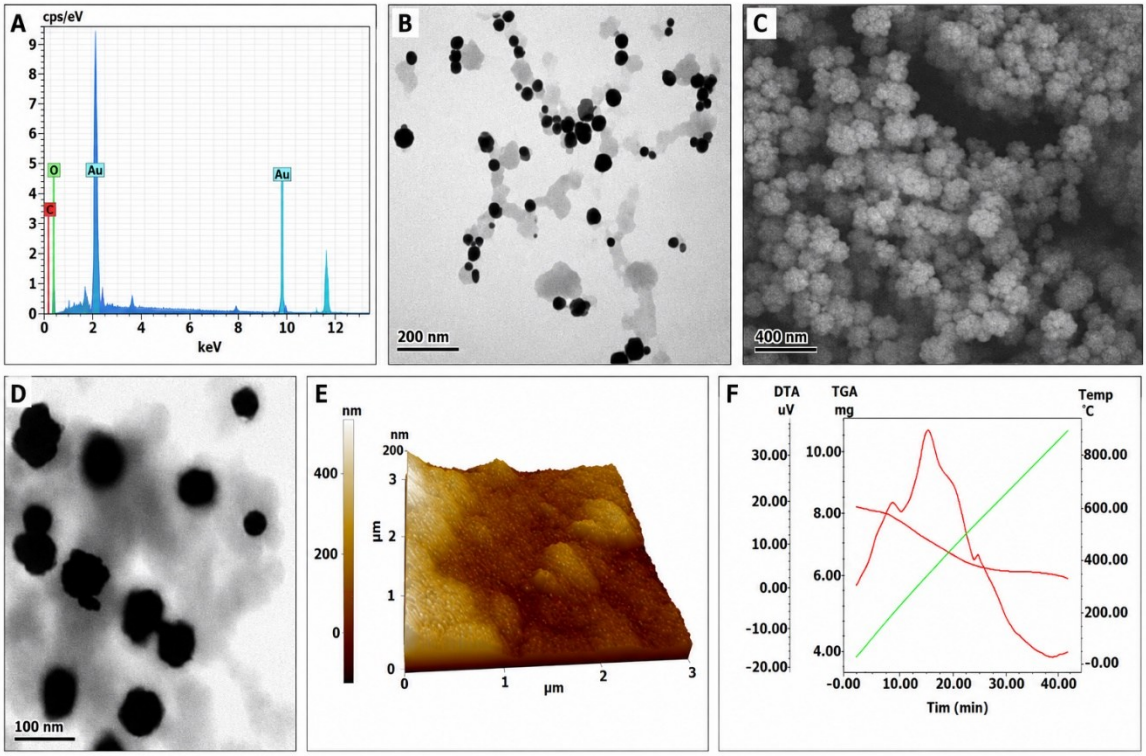

Fig. 4. Comprehensive elemental profiling, morphological attributes, and thermal degradation behavior of the green-synthesized Au NPs mediated by pomegranate peel extract: (a) EDX spectrum, (b) TEM microphotograph, (c) FESEM image, (d) STEM micrograph, (e) AFM topographic scan, and (f) TGA-DTG thermogram

The EDX data in Fig. 4a were used to determine the elemental composition of the nanoparticles. The strong peaks in the profile confirmed the formation of Au NPs. Additionally, minor carbon (C) and oxygen (O) peaks were observed. These peaks represent the phytochemical components that cap the Au NPs (Doan *et al.* 2020; Chen *et al.* 2021; Hosny *et al.* 2021; Mandhata *et al.* 2021; Rosyidah *et al.* 2024).

Figure 4f illustrates the TGA-DTG analysis of the synthesized Au NPs up to 1000 °C. The thermogram revealed a four-step weight loss process. The first, second, third, and fourth mass losses were 3.0%, 13.9%, 20.1%, and 8.8%, respectively. The initial weight loss occurred between 24.5 and 207.3 °C due to the removal of adsorbed water. The subsequent mass losses in the ranges of 206.4 to 583.6 °C and 583.6 to 876.6 °C were caused by the decomposition of bioorganic compounds. These stages confirm the thermal degradation of the phytochemical coating encapsulating the nanoparticles (Baran 2025).

Antimicrobial Effects of Au NPs

Antibiotic resistance among microorganisms is a global problem. It emerges due to unplanned and inconsistent antibiotic usage. Various scientific studies have addressed this issue. Metal nanoparticles have been shown to overcome this challenge (Scarafile 2016; Nishanthi *et al.* 2019; Nieto-Argüello *et al.* 2022). The minimum inhibitory concentrations (MIC) of the synthesized Au NPs were determined using the microdilution method. The nanoparticles were tested against pathogenic Gram-negative bacteria, Gram-positive bacteria, and *C. albicans*. The synthesized Au NPs, standard antibiotics, and the $HAuCl_4$ solution were evaluated under identical conditions for each strain. Concentrations between 0.32 and 0.78 µg/mL significantly inhibited the growth of Gram-positive bacteria. The lowest MIC values were observed against *C. albicans*, *B. subtilis*, and *E. coli* at doses of 0.36, 0.78, and 0.32 µg/mL, respectively. The remaining strains were also successfully suppressed. Notably, the required inhibitory doses for the Au NPs were significantly lower than those of the $HAuCl_4$ solution and standard antibiotics (Table 1).

Table 1. MIC Values of Synthesized Au NPs, Antibiotics, and $HAuCl_4$ Solution

Microorganisms	Au NPs (µg/mL)	$HAuCl_4$ Solution (µg/mL)	Antibiotic* (µg/mL)
C. albicans	0.36 ± 0.02	16.00 ± 2.49	1.00 ± 0.16
E. coli	0.78 ± 0.03	8.00 ± 1.63	2.00 ± 0.33
B. subtilis	0.32 ± 0.02	16.00 ± 1.63	1.00 ± 0.13

Note: The data display the antibacterial effects on microbial growth (n = 3, $\bar{X} \pm S\bar{x}$);
*__Flucanozol__ was used on *C. albicans*, __vancomycin__ was used on *B. subtilis*, and __colistin__ was used on *E. coli*

The antimicrobial activity of Au NPs depends on parameters including surface charge, size, and concentration. Microorganisms generally have a net negative surface charge. Therefore, they interact with ionized, positively charged nanoparticles through electrostatic attraction. This interaction with Au NPs directly alters the membrane potential of the microorganisms. Additionally, Au NPs disrupt energy metabolism by suppressing ATPase function. This suppression leads to a significant decrease in cellular

ATP levels (Baran 2025). Furthermore, Au nanoparticles upregulate the expression of genes associated with redox processes. This upregulation increases reactive oxygen species (ROS) production. Elevated ROS levels cause functional and structural damage to critical systems including energy metabolism. Consequently, microorganisms die due to these severe disruptions in biological systems (Fig. 5) (Arshad *et al.* 2024; Baran 2025).

The synthesized Au NPs exhibit high stability due to their negative surface charge. Their spherical morphology below 100 nm holds significant value for medical applications. These synthesized Au NPs provide crucial insights into nanoparticle-microorganism interactions. Therefore, they can highly advance the development of novel antimicrobial agents.

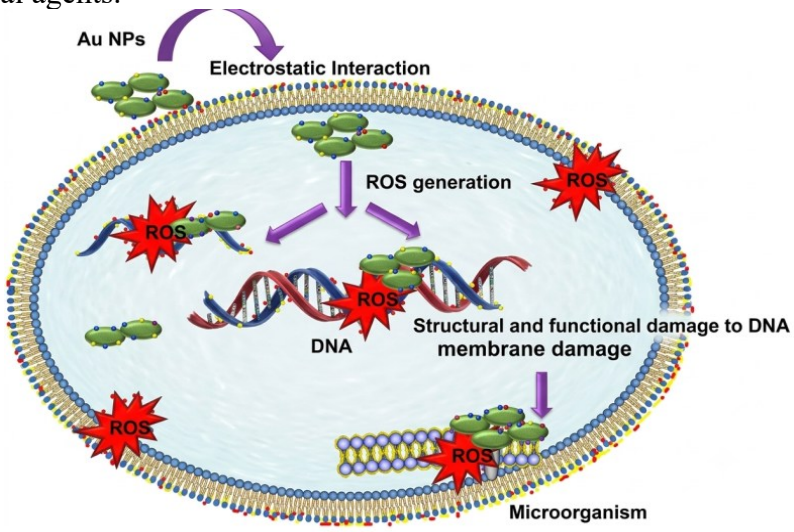

Fig. 5. Illustration depicting the approach by which Au NPs have antibacterial effects on microorganisms

The antimicrobial properties of Au NPs generated through green synthesis utilising the Micro dilution technique were found to be efficient against *Escherichia coli*, *Bacillus subtilis*, and *Candida albicans* at concentrations ranging from 2.5 to 50 µg/mL (Rambau *et al.* 2024; Sharifi-Rad *et al.* 2024).

Anticancer Effects of Au NPs

The cytotoxic effects of Au NPs synthesized from pomegranate agricultural waste were evaluated using the MTT assay. The study investigated the viability reduction of healthy cells (HDF) and cancer cells (CaCo-2, U118, and Skov-3) induced by these nanoparticles. Table 2 and Fig. 6 demonstrate that the Au NPs were highly effective against Skov-3 and CaCo-2 cancer cells. At a concentration of 25 µg/mL, the inhibition percentages reached 93.6% and 85.5%, respectively. At the same dose, the viability of U118 cells decreased 37.4%. The U118 cancer cells exhibited their highest inhibition of 92.72% at a dose of 200 µg/mL. However, this high concentration also suppressed healthy cells by 81.5%. The CaCo-2 cells were most efficiently targeted at a concentration of 50 µg/mL. This concentration was determined as the most effective dose against these specific cancer cells. Notably, the inhibitory effect on healthy cells at this dosage was reported to be negligible.

Table 2. Inhibition Percentages of Cell Line Viability Induced by the Toxic Effects of Au NPs

Cell Lines	25 µg mL^{-1}	50 µg mL^{-1}	100 µg mL^{-1}	200 µg mL^{-1}
HDF	33.18 ± 0.008	32.63 ± 0.012	33.59 ± 0.003	44.71 ± 0.023
U118	15.63 ± 0.015	20.83 ± 0.032	21.43 ± 0.066	24.96 ± 0.061
CaCo-2	26.14 ± 0.001	45.36 ± 0.012	60.68 ± 0.030	65.57 ± 0.28
Skov-3	28.10 ± 0.003	36.85 ± 0.003	41.65 ± 0.006	47.64 ± 0.061

The data displays the calculated percent inhibition rates (n = 3, $\overline{X}$ ± $S\overline{x}$; 24 h)

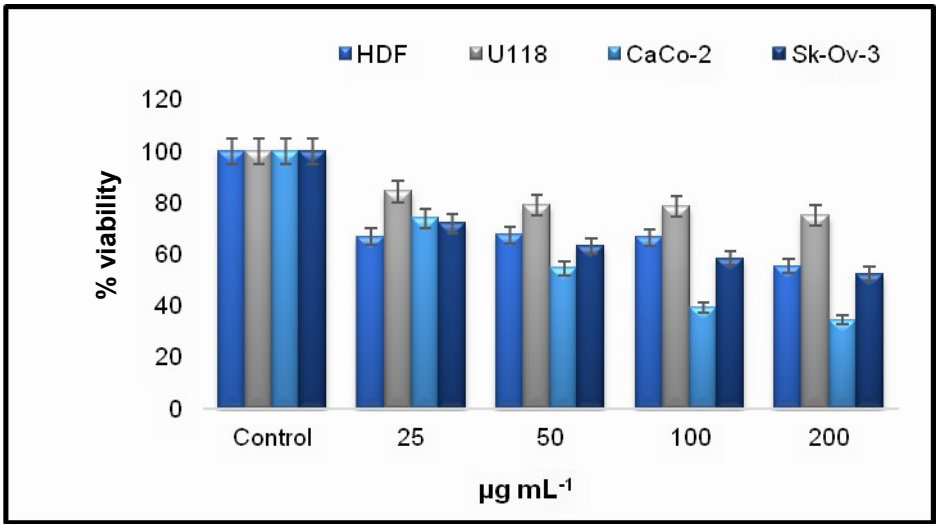

Fig. 6. Percent viability suppressive effect concentrations of Au NPs on healthy cell HDF and cancer cells, Skov-3, CaCo-2, and U118

Cancer remains a major cause of global mortality. Extensive research has focused on developing novel anticancer agents for this debilitating disease. Nanoparticle toxicity depends on concentration, shape, size, exposure time, and surface charge. These properties dictate the severity of the cytotoxic effect (Baran 2025). Tumor progression requires hypervascular structures for nutrient supply. These leaky vessels have wide gaps that allow nanoparticles to accumulate at target sites (Chen *et al.* 2021; Oliveira *et al.* 2024). Due to their dimensions, Au NPs easily penetrate cell membranes. Inside cells, Au NPs induce reactive oxygen species (ROS) production and activate caspases to trigger apoptosis. This process disrupts mitochondrial permeability and stimulates cytochrome c release. Consequently, these cellular damages generate signaling cascades leading to programmed cell death (Fig. 7) (Al-Radadi *et al.* 2024; Baran 2025).

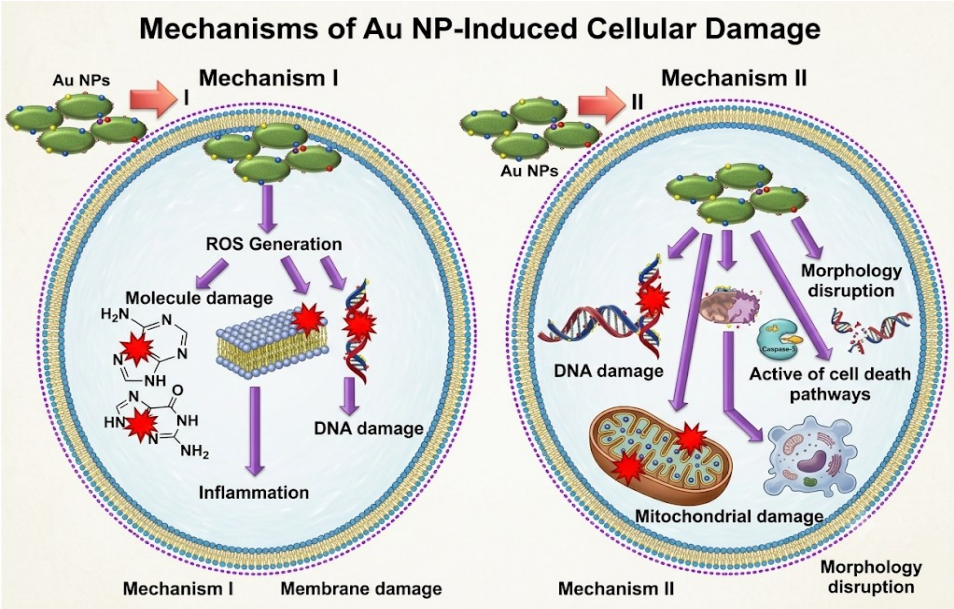

Fig. 7. Illustration depicting the approach by which Au NPs have anticancer effects on cancer cells

CONCLUSIONS

Environmentally friendly technologies for the synthesis of metal nanoparticles have attracted increasing attention as sustainable alternatives to conventional chemical methods. In this study, gold nanoparticles (AuNPs) were successfully synthesized using pomegranate agricultural waste extract through a green synthesis approach. This eco-friendly strategy offers several advantages, including rapid synthesis, cost-effectiveness, reduced energy consumption, a short extraction process, and the utilization of a centralized waste management system, thereby contributing to sustainable nanoparticle production.

The synthesized AuNPs were characterized using UV–Vis spectroscopy, FE-SEM, TEM, EDX, XRD, AFM, FTIR, and TGA-DTA analyses. The characterization results confirmed the successful formation of AuNPs, exhibiting a characteristic surface plasmon resonance (SPR) peak at 532.6 nm. Dynamic light scattering analysis revealed an average hydrodynamic diameter of 47.1 nm, while zeta potential measurements demonstrated a negative surface charge of −16.2 mV, indicating moderate colloidal stability. Electron microscopy analyses further confirmed that the nanoparticles possessed a predominantly spherical morphology.

The biological activities of the synthesized AuNPs were evaluated against pathogenic microorganisms and human cancer cell lines using broth microdilution and MTT assays. The nanoparticles exhibited remarkable antimicrobial activity at concentrations ranging from 0.32 to 0.36 μg mL^{-1}, which were substantially lower than those required for conventional antibiotics. Furthermore, AuNP concentrations between 25 and 200 μg mL^{-1} significantly inhibited the proliferation of SKOV-3, Caco-2, and U118 cancer cell lines. Among the tested concentrations, 50 μg mL^{-1} demonstrated the most favorable therapeutic profile by providing pronounced anticancer activity while maintaining comparatively lower cytotoxicity toward healthy cells.

Overall, the biosynthesized AuNPs exhibited potent antibacterial, antifungal, and anticancer activities even at relatively low concentrations. These findings highlight the potential of pomegranate agricultural waste as a sustainable and value-added resource for the green production of biocompatible gold nanoparticles. The synthesized AuNPs represent promising candidates for future biomedical applications and provide a strong foundation for the development of novel antimicrobial and anticancer nanotherapeutic agents. Nevertheless, further in vivo, pharmacokinetic, toxicological, and clinical studies are required to fully establish their safety and therapeutic efficacy before clinical translation.

ACKNOWLEDGEMENTS

Conflict of Interest

The authors declare no conflict of interest.

REFERENCES CITED

Adem, Z., Bekana, D., Temesgen, A., Teju, E., Amde, M., and Jabesa, A. (2024). "Plasmon-based colorimetric assay using green synthesized gold nanoparticles for the detection of bisphenol A," *Anal. Sci.* 40(4), 671-679. https://doi.org/10.1007/s44211-023-00500-8

Al-Radadi, N. S. (2023). "Ephedra mediated green synthesis of gold nanoparticles (AuNPs) and evaluation of its antioxidant, antipyretic, anti-asthmatic, and antimicrobial properties," *Arab. J. Chem* 16(1), article 104353. https://doi.org/10.1016/j.arabjc.2022.104353

Al-Radadi, N. S., AlBishri, W. M., ElShebiney, S. A., and Salem, N. A. (2024). "Plant-mediated green synthesis of gold nanoparticles using an aqueous extract of *Passiflora ligularis*, optimization, characterizations, and their neuroprotective effect on propionic acid-induced autism in Wistar Rats," *Saudi Pharm. J.* 32(2), article 101921. https://doi.org/10.1016/j.jsps.2023.101921

Al-Zoreky, N. S. (2009). "Antimicrobial activity of pomegranate (*Punica granatum* L.) fruit peels," *Int. J. Food Microbiol.* 134(3), 244-248. https://doi.org/10.1016/j.ijfoodmicro.2009.07.002

Arshad, F., Naikoo, G. A., Hassan, I. U., Chava, S. R., El-Tanani, M., Aljabali, A. A., and Tambuwala, M. M. (2024). "Bioinspired and green synthesis of silver nanoparticles for medical applications: A green perspective," *Appl. Biochem. Biotechnol.* 196(6), 3636-3669. https://doi.org/10.1007/s12010-023-04719-z

Baran, A. (2023). "Inhibitory effects of gold nanoparticles biosynthesized by redox reaction using *Rheum ribes* lam fruit peels on pathogen strains and cancer cells," *Part. Sci. Technol.* 41(7), 978-989. https://doi.org/10.1080/02726351.2023.2164875

Baran, A. (2025). "A study to assess the pharmacological agent potential of gold nanoparticles and their effects on human cancer cells and hospital pathogens using *in vitro* methods," *Front. Pharmacol.* 15, article 1498734. https://doi.org/10.3389/fphar.2024.1498734

Chen, J., Li, Y., Fang, G., Cao, Z., Shang, Y., Alfarraj, S., Ali Alharbi, S., Duan, X., Yang, S., and Li, J. (2021). "Green synthesis, characterization, cytotoxicity,

antioxidant, and anti-human ovarian cancer activities of *Curcumae kwangsiensis* leaf aqueous extract green-synthesized gold nanoparticles," *Arab. J. Chem.* 14(3), article 103000. https://doi.org/10.1016/j.arabjc.2021.103000

De O. Trovão, L., Dos S. Rodrigues, L., Mendes, P. M., Alves, P. C. S., Da S. Oliveira, A., Brito, J. M., Vale, A. A. M., Dimitrius, D. V., Simão, G., Dos Santos, A. P. S. A., *et al.* (2023). "The immunomodulatory activity of *Punica granatum* L. peel extract increases the lifespan of mice with lethal sepsis," *J. Immunol. Res.* 2023(1), article 2868707 https://doi.org/10.1155/2023/2868707

Doan, V. D., Thieu, A. T., Nguyen, T. D., Nguyen, V. C., Cao, X. T., Nguyen, T. L. H., and Le, V. T. (2020). "Biosynthesis of gold nanoparticles using *Litsea cubeba* fruit extract for catalytic reduction of 4-nitrophenol," *J. Nanomater*. 2020(1), article 4548790. https://doi.org/10.1155/2020/4548790

Döll, E. G., Santana, E. R., Winiarski, J. P., Baumgarten, L. G., and Vieira, I. C. (2023). "Green synthesis of gold nanoparticles using peach extract incorporated in graphene for the electrochemical determination of antioxidant butylated hydroxyanisole in food matrices," *Biosensors* 13(12), article 1037. https://doi.org/10.3390/bios13121037

Dubey, S. P., Dwivedi, A. D., Lahtinen, M., Lee, C., Kwon, Y. N., and Sillanpaa, M. (2013). "Protocol for development of various plants leaves extract in single-pot synthesis of metal nanoparticles," *Spectrochim. Acta A- Mol. Biomol. Spectrosc.* 103, 134-142. https://doi.org/10.1016/j.saa.2012.11.021

Franzolin, M. R., Courrol, S., Rodrigues, F., Silva, D. O., and Courrol, L. C. (2022). "Antimicrobial activity of silver and gold nanoparticles prepared by photoreduction process with leaves and fruit extracts of *Plinia cauliflora* and *Punica granatum*," *MDPI Mol.* 27, article 6860. https://doi.org/https://doi.org/10.3390/molecules27206860

Hosny, M., Fawzy, M., El-Borady, O. M., and Mahmoud, A. E. D. (2021). "Comparative study between *Phragmites australis* root and rhizome extracts for mediating gold nanoparticles synthesis and their medical and environmental applications," *Adv. Powder Technol.* 32(7), 2268-2279. https://doi.org/10.1016/j.apt.2021.05.004

İpek, P., Baran, M. F., Baran, A., Hatipoğlu, A., Keskin, C., Yildiztekin, M., Küçükaydın, S., Becerikli, H., Kurt, K., Eftekhari, A., *et al.* (2024). "Green synthesis and evaluation of antipathogenic, antioxidant, and anticholinesterase activities of gold nanoparticles (Au NPs) from *Allium cepa* L. peel aqueous extract," *Biomass Convers. Biorefin.* 14(9), 10661-10670.

Irtegun Kandemir, S., and İpek, P. (2018). "Antiproliferative effect of *Potentilla fulgens* on glioblastoma cancer cells through downregulation of Akt/mTOR signaling pathway," *J. Cancer Res. Ther.* 14(7), 1525-1534. https://doi.org/10.4103/jcrt.JCRT

Kharey, P., Goel, M., Husain, Z., Gupta, R., Sharma, D., M, M., Palani, I. A., and Gupta, S. (2023). "Green synthesis of biocompatible superparamagnetic iron oxide-gold composite nanoparticles for magnetic resonance imaging, hyperthermia and photothermal therapeutic applications," *Mater. Chem. Phys.* 293, article 126859. https://doi.org/10.1016/j.matchemphys.2022.126859

Kumar, P. S., Jeyalatha, M. V., Malathi, J., and Ignacimuthu, S. (2018). "Anticancer effects of one-pot synthesized biogenic gold nanoparticles (Mc-AuNps) against laryngeal carcinoma," *J. Drug Deliv. Sci. Technol.* 44(18), 118-128. https://doi.org/10.1016/j.jddst.2017.12.008

Li, R., Chen, X., Ye, H., and Sheng, X. (2024). "Green synthesis of gold nanoparticles from the extract of *Crocus sativus* to study the effect of antidepressant in adolescence

and to observe its aggressive and impulsive behavior in rat models," *S. Afr. J. Bot.* 165, 455-465. https://doi.org/10.1016/j.sajb.2023.12.029

Mandhata, C. P., Sahoo, C. R., Mahanta, C. S., and Padhy, R. N. (2021). "Isolation, biosynthesis and antimicrobial activity of gold nanoparticles produced with extracts of *Anabaena spiroides*," *Bioprocess. Biosyst. Eng.* 44(8), 1617-1626. https://doi.org/10.1007/s00449-021-02544-4

Negi, P. S., and Jayaprakasha, G. K. (2003). "Antioxidant and antibacterial activities of *Punica granatum* peel extracts," *J. Food Sci* 68(4), 1473-1477. https://doi.org/10.1111/j.1365-2621.2003.tb09669.x

Niaz, S., Khan, S., Khan, H. N., Ullah, I., Anjum, K., Shahzad, N. S., and Saira, N. (2026). "Plant-mediated green synthesis of gold nanoparticles using pomegranate peel (*Punica granatum* L) extract: Free radical scavenging, drug loading and photo-catalytic activity," *J. Sol-Gel Sci. Technol.* 118(36), 1-6. https://doi.org/10.1007/s10971-025-07016-9.

Nieto-Argüello, A., Medina-Cruz, D., Pérez-Ramírez, Y. S., Pérez-García, S. A., Velasco-Soto, M. A., Jafari, Z., De Leon, I., González, M. U., Huttel, Y., Martínez, L., *et al.* (2022). "Composition-dependent cytotoxic and antibacterial activity of biopolymer-capped Ag/Au bimetallic nanoparticles against melanoma and multidrug-resistant pathogens," *Nanomaterials* 12(5), article 779. https://doi.org/10.3390/nano12050779

Nishanthi, R., Malathi, S., Paul, J. S., and Palani, P. (2019). "Green synthesis and characterization of bioinspired silver, gold and platinum nanoparticles and evaluation of their synergistic antibacterial activity after combining with different classes of antibiotics," *Mater. Sci. Eng. C* 96, 693-707. https://doi.org/10.1016/j.msec.2018.11.050

Niżnik, Ł., Noga, M., Kobylarz, D., Frydrych, A., Krośniak, A., Kapka-Skrzypczak, L., and Jurowski, K. (2024). "Gold nanoparticles (AuNPs)—Toxicity, safety and green synthesis: A critical review," *Int. J. Mol. Sci.* 25(7), article 4057. https://doi.org/10.3390/ijms25074057

Oliveira, M., Sousa, A., Sá, S., Soares, S., Pereira, A. C., Rocha, A. C., Pais, P., Ferreira, D., Almeida, C., Luís, C., *et al.* (2024). "Harvesting the power of green synthesis: Gold nanoparticles tailored for prostate cancer therapy," *Int. J. Mol. Sci.* 25(4), article 2277. https://doi.org/10.3390/ijms25042277

Pechprakob, W., Prasopsuk, V., and Danwanichakul, P. (2023). "Photocatalytic activity of gold and silver nanoparticles synthesized by using coffee flower extract," *Sci. Technol. Asia* 28(4), 191-202.

Rambau, U., Masevhe, N. A., and Samie, A. (2024). "Green synthesis of gold and copper nanoparticles by *Lannea discolor*: Characterization and antibacterial activity," *Inorganics* 12(2), article 36. https://doi.org/10.3390/inorganics12020036

Rosyidah, A., Purbani, D. C., Pratiwi, R. D., Muttaqien, S. E., Nantapong, N., Warsito, M. F., Fikri, M. N., Ruth, F., Gustini, N., Syahputra, G., *et al.* (2024). "Eco-friendly synthesis of gold nanoparticles by marine microalgae *Synechococcus moorigangae*: Characterization, antimicrobial, and antioxidant properties," *Kuwait J. Sci.* 51(2), article 100194. https://doi.org/10.1016/j.kjs.2024.100194

Scaglione, E., Sateriale, D., Mantova, G., Di Rosario, M., Continisio, L., Vitiello, M., Pagliarulo, C., Colicchio, R., Pagliuca, C., and Salvatore, P. (2024). "Antimicrobial efficacy of *Punica granatum* Lythraceae peel extract against pathogens belonging to the ESKAPE group," *Front Microbiol* 15, article 1383027.

https://doi.org/10.3389/fmicb.2024.1383027
Scarafile, G. (2016). "Antibiotic resistance: Current issues and future strategies," *Rev. Health Care* 7(1), 3-16. https://doi.org/10.7175/rhc.v7i1.1226
Serdar, G. (2024). "Biosynthesis and characterization of gold nanoparticles using microwave-assisted technology from pomegranate (*Punica granatum* L .) leaf extract produced by the method of supercritical fluid extraction (SFE)," *Plasmonics* 2024, 2233-2243. https://doi.org/10.1007/s11468-024-02312-6
Sharifi-Rad, M., Kishore Mohanta, Y., Pohl, P., Nayak, D., and Messaoudi, M. (2024). "Facile phytosynthesis of gold nanoparticles using *Nepeta bodeana* Bunge: Evaluation of its therapeutics and potential catalytic activities," *J. Photochem. Photobiol. A- Chem.* 446, article 115150. https://doi.org/10.1016/j.jphotochem.2023.115150
Suriyakala, G., Sathiyaraj, S., Babujanarthanam, R., Alarjani, K. M., Hussein, D. S., Rasheed, R. A., and Kanimozhi, K. (2022). "Green synthesis of gold nanoparticles using *Jatropha integerrima* Jacq. flower extract and their antibacterial activity," *J. King Saud Univ. Sci.* 34(3), article 101830. https://doi.org/10.1016/j.jksus.2022.101830
Ullah, I., Rauf, A., Khalil, A. A., Luqman, M., Islam, M. R., Hemeg, H. A., Ahmad, Z., Al-Awthan, Y. S., Bahattab, O., and Quradha, M. M. (2024). "*Peganum harmala* L. extract-based gold (Au) and silver (Ag) nanoparticles (NPs): Green synthesis, characterization, and assessment of antibacterial and antifungal properties," *Food Sci. Nutr.* 12(6), 4459-4472. https://doi.org/10.1002/fsn3.4112
Valero-Mendoza, A. G., Meléndez-Rentería, N. P., Chávez-González, M. L., Flores-Gallegos, A. C., Wong-Paz, J. E., Govea-Salas, M., Zugasti-Cruz, A., and Ascacio-Valdés, J. A. (2023). "The whole pomegranate (*Punica granatum* L), biological properties and important findings: A review," *Food Chem. Adv.* 2, article 100153. https://doi.org/10.1016/j.focha.2022.100153
Xie, W., Zhang, Y., Yang, X., Yu, P., and Ban, D. (2024). "Green synthesis of gold nanoparticles mediated by extract of *Curcuma longa* under ultrasonic condition: Investigation of its application for reduction of dye pollutants and repairing the articular cartilage in an animal model of osteoarthritis of the knee," *Inorg. Chem. Commun.* 162, article 112169. https://doi.org/10.1016/j.inoche.2024.112169
Zahin, M., Aqil, F., and Ahmad, I. (2010). "Broad spectrum antimutagenic activity of antioxidant active fraction of *Punica granatum* L. peel extracts," *Mutat. Res. Genet. Toxicol. Environ. Mutagen.* 703(2), 99-107. https://doi.org/10.1016/j.mrgentox.2010.08.001

Article submitted: June 3, 2026; Peer review completed: July 18, 2026; Revised version received and accepted: July 30; Published: August 24, 2026.
DOI: 10.15376/biores.21.4.9947-9961